# Stationary wave patterns generated by an impurity moving with supersonic velocity through a Bose-Einstein condensate

T.-L. Horng,[1] S.-C. Gou,[2] T.-C. Lin,[3] G. A. El,[4] A. P. Itin,[5,6] and A. M. Kamchatnov[7]

[1]*Department of Applied Mathematics, Feng Chia University, Taichung 40724, Taiwan*

[2]*Department of Physics, National Changhua University of Education, Changhua 50058, Taiwan*

[3]*Department of Mathematics, National Taiwan University, Taipei, 10617, Taiwan*

[4]*Department of Mathematical Sciences, Loughborough University, Loughborough LE11 3TU, United Kingdom*

[5]*Department of Applied Physics, Helsinki University of Technology, P.O. Box 5100, 02015, Finland*

[6]*Space Research Institute, Russian Academy of Sciences, Moscow, 117997, Russia*

[7]*Institute of Spectroscopy, Russian Academy of Sciences, Troitsk, Moscow Region 142190, Russia*

Formation of stationary three-dimensional (3D) wave patterns generated by a small pointlike impurity moving through a Bose-Einstein condensate with supersonic velocity is studied. Asymptotic formulae for a stationary far-field density distribution are obtained. Comparison with the three-dimensional numerical simulations demonstrates that these formulae are accurate enough already at the distances from the obstacle equal to a few wavelengths.

## I. INTRODUCTION

As is well known, superfluidity means that slow-enough flow of a fluid is not accompanied by heat production or generation of excitations of any kind. As a result, the motion of a fluid is free of dissipation. In a similar way, the motion of an impurity through a superfluid goes on without any friction for small-enough values of its velocity. The threshold velocity above which superfluidity is lost is determined by various physical mechanisms depending on the nature of the fluid and the geometry of the process. For example, in the original Landau theory [1,2] of superfluidity it breaks down when the generation of rotons becomes possible which leads to the famous Landau criterion for superfluidity. However, Landau's estimate for this mechanism of dissipation gives too large threshold velocity for HeII, and this disagreement with the theory was explained by Feynman [3] by the possibility of the generation of vortex rings. This phenomenon is essential for large-enough obstacles with the size about the healing length. In Bose-Einstein condensates (BECs) of rarefied gases the healing length can be relatively large and the generation of vortices by small impurities becomes ineffective. In this case the BEC remains superfluid for all velocities less than the minimal sound velocity corresponding to the long wavelength limit of the Bogoliubov dispersion law. For the supersonic motion of an impurity, the Cherenkov radiation of sound waves is the main mechanism of the appearance of friction and the corresponding "drag force" was calculated in [4,5].

However, the detailed wave pattern generated by a moving impurity is also of considerable interest. This problem became very topical in two-dimensional (2D) case in connection with the results of the experiment [6,7] in which the waves were generated by the flow of a condensate expanding through an obstacle created by a laser beam. Similar structures have been also observed recently in a superfluid flow of polaritons in semiconductor microcavities [8]. The obstacles in these systems have the size comparable with or greater

than the healing length, so the arising wave pattern here can be quite complicated. Already in the numerical experiment [9], which modeled a similar situation, it was noticed that the interference of sound (Bogoliubov) waves yields the wave pattern located outside the Mach cone. Analytic theory of such wave patterns was developed in [7,10,11]. In many respects, this theory is analogous to the well-known Kelvin's theory of "ship waves" generated by a ship moving in still deep water, with the dispersion law for the surface water waves replaced by the Bogoliubov dispersion law for sound waves in BEC. Besides that, due to a large size of the laser beam, vortices or oblique dark solitons located inside the Mach cone can also be generated by a 2D flow of a BEC. The corresponding theory was developed in [12–14] and was recently generalized [15] for a two-component condensate. However, analogous theory for a three-dimensional (3D) flow has not been developed yet, although it is of considerable interest for the understanding of the wave processes in BECs (see, e.g., [16]). In this paper, we shall consider both analytically and numerically the 3D wave pattern created by a small impurity moving with supersonic velocity through a bulk Bose-Einstein condensate. Here we limit ourselves to the case of a uniform condensate, which implies that the characteristic size of the structure is much less than the size of the condensate confined in a trap. Besides that, we assume that the size of the obstacle does not exceed the healing length and, hence, one can neglect the nonlinear structures generated inside the Mach cone.

## II. STATIONARY WAVE PATTERN

Dynamics of BEC of rarefied gases is described very well by the Gross-Pitaevskii (GP) equation

$$i\psi_t + \frac{1}{2}\Delta\psi + (1 - |\psi|^2)\psi - V\psi = 0, \qquad (1)$$

which is written here in standard nondimensional notation (see, e.g., [11]) so that the density of an undisturbed BEC

with the repulsive interaction between atoms is equal to unity. We suppose that the external potential $V$ is created by a pointlike impurity moving with the velocity **U** along the $x$ axis in negative direction,

$$V(\mathbf{r}) = V_0 \delta(\mathbf{r} + \mathbf{U}t). \qquad (2)$$

The stationary wave pattern can be obtained for a supersonic velocity **U** which in our nondimensional units with the sound velocity equal to unity means

$$|\mathbf{U}| \equiv M > 1, \qquad (3)$$

with $M$ being the Mach number. Assuming that the interaction with the impurity is weak, we can apply the perturbation theory [4,5,11] and linearize Eq. (1) with respect to a small disturbance $\delta\Psi$ of the wave function, $\Psi = 1 + \delta\Psi$. Then $\delta\Psi$ satisfies the equation

$$i\delta\Psi_t + \frac{1}{2}\Delta\delta\Psi - (\delta\Psi + \delta\Psi^*) - V_0\delta(\mathbf{r} + \mathbf{U}t) = 0, \qquad (4)$$

which can be readily solved by the Fourier method and the resulting perturbation of density $\delta n = \delta|\Psi|^2 \cong \delta\Psi + \delta\Psi^*$ is given by the expression (see, e.g., Eq. 20 in [11])

$$\delta n = V_0 \int \frac{k^2 e^{i\mathbf{k}\cdot\mathbf{r}}}{(\mathbf{k}\cdot\mathbf{U})^2 - k^2(1 + k^2/4) + i\varepsilon} \frac{d^3k}{(2\pi)^3}, \qquad (5)$$

where $\varepsilon = 8M\delta\cos\eta/k$ is an infinitely small parameter, $\delta \to 0$, which determines the rule of going around the poles of the integrand function. Actually, this perturbation theory is analogous to the well-known quantum-mechanical Born's method in momentum representation applied to Eq. (4).

Since the wave pattern is axially symmetric with respect to the $x$ axis, it is convenient to define the coordinate system so that the observation point lies in the $(x,y)$ plane. Then vector **r** has the components

$$\mathbf{r} = (r\cos\chi, r\sin\chi, 0), \qquad (6)$$

where $\chi$ is the polar angle between **r** and the $x$ axis. Let the vector **k** lie in the plane making an angle $\phi$ with the $(x,y)$ plane. Then its components can be parameterized as

$$\mathbf{k} = (-k\cos\eta, k\sin\eta\cos\phi, k\sin\eta\sin\phi), \qquad (7)$$

where $k\cos\eta$ is the projection of the vector **k** on the $x$ axis. A schematic picture showing the angles $\eta$, $\chi$, and $\mu = \pi - \eta - \chi$ can be found in Fig. 1.

Substitution of Eqs. (6) and (7) into Eq. (5) and simple transformations cast this expression to the form

$$\delta n = \frac{V_0}{\pi^2} \int_0^\infty \int_0^\pi \frac{k^2 \sin\eta J_0(kr\sin\eta\sin\chi)e^{-ikr\cos\eta\cos\chi}}{k^2 - k_0^2 - i\varepsilon} dk d\eta, \qquad (8)$$

where

$$k_0 = 2\sqrt{M^2\cos^2\eta - 1}, \qquad (9)$$
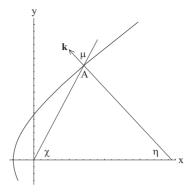
and we have used the well-known integral representation



FIG. 1. Coordinates defining the radius vector **r** and the wave vector **k**. The latter is normal to the wave crest line of the ship wave which is shown schematically by a curve.

$$J_0(z) = \frac{1}{2\pi}\int_0^{2\pi} e^{iz\cos\phi}d\phi \qquad (10)$$

for the Bessel function.

The integral in Eq. (8) can be estimated by the method similar to that used in Ref. [11]. First, reality of $\delta n$ enables one to represent Eq. (8) as a half-sum of this expression and its complex conjugate, and to make the replacements $\mathbf{k} \to -\mathbf{k}$, $\varepsilon \to -\varepsilon$ in one of integrals. As a result we get

$$\delta n = \frac{V_0}{2\pi^2}\int_0^\pi d\eta \sin\eta$$

$$\times \int_{-\infty}^\infty \frac{k^2 J_0(kr\sin\eta\sin\chi)e^{-ikr\cos\eta\cos\chi}}{k^2 - k_0^2 - i\varepsilon}dk, \qquad (11)$$

where $k$ integration takes place over the whole $k$ axis. Taking into account definition of $\varepsilon = 8M\delta\cos\eta/k$, we find that the integrand function has three poles,

$$k = \pm k_0 + \frac{4M\delta\cos\eta}{k_0^2}i, \quad k = -\frac{8M\delta\cos\eta}{k_0^2}i; \qquad (12)$$

the first two are located in the upper complex half-plane and the third one is in the lower complex half-plane for $\cos\eta > 0$ which corresponds to the region outside the Mach cone. Hence, we can calculate this integral if we close the contour of integration by an infinitely large half-circle $k = |k|e^{i\theta}$ with either $0 \le \theta \le \pi$ or $\pi \le \theta \le 2\pi$, provided that the contribution of these additional paths of integration vanishes as $|k| \to \infty$.

To analyze the behavior of these integrals as $|k| \to \infty$, we use an asymptotic expression for the Bessel function,

$$J_0(z) \approx \sqrt{\frac{2}{\pi z}}\cos\left(z - \frac{\pi}{4}\right), \quad z \gg 1. \qquad (13)$$

Hence, Eq. (11) can be represented as a sum of two integrals with the integrand functions having the exponential factors

$$\exp[-ikr\cos(\eta \pm \chi) - \pi/4]. \qquad (14)$$

If $\cos(\chi \pm \eta) > 0$, then this factor decays exponentially in the lower complex $k$ half-plane, we close the contour by a lower half-circle, and since the residue of the third pole [Eq. (12)]

located inside this contour is equal to zero, the integral vanishes in this case. On the contrary, if

$$\cos(\chi \pm \eta) < 0, \tag{15}$$

then we close the contour of integration in the upper half-plane and both poles give nonzero contributions into the integral. Thus, we get

$$\delta n = \frac{V_0}{\pi} \int_0^\pi k \sin \eta \sin(kr \cos \chi \cos \eta) J_0(kr \sin \chi \sin \eta) d\eta, \tag{16}$$

where $k$ is defined by Eq. (9); i.e., we have dropped out the index for convenience of notation.

In the far-field region $kr \gg 1$ we replace the Bessel function by its asymptotic expression [Eq. (13)] to obtain

$$\delta n = \frac{V_0}{\pi} \sqrt{\frac{k \sin \eta}{\sin \chi}} \int_0^\pi [e^{ikr \cos(\chi+\eta)+\pi/4} + e^{ikr \cos(\chi-\eta)-\pi/4}] d\eta. \tag{17}$$

These integrals can be calculated by the method of stationary phase. The stationary point of the phase,

$$s_1 = k \cos(\chi + \eta), \tag{18}$$

is determined by the equation $ds_1/d\eta = 0$ which gives the relation between the angles $\chi$ and $\eta$,

$$\tan(\chi + \eta) = -\frac{2M^2}{k^2} \sin 2\eta \tag{19}$$

or

$$\tan \chi = \frac{(1 + k^2/2) \tan \chi}{M^2 - (1 + k^2/2)}. \tag{20}$$

This expression coincides with the results obtained in the case of 2D obstacle [10,11] and satisfies condition (15). On the contrary, the second term in Eq. (17) with the phase $s_2 = k \cos(\chi - \eta)$ leads to the relation between $\chi$ and $\eta$ which is excluded by Eq. (15). Hence we take into account the first term only and reduce this integral into the Gaussian one around the vicinity of the stationary point. As a result we obtain the following distribution of the density in the wave pattern:

$$\delta n = \frac{2V_0}{\pi r} \frac{\{[M^2(M^2 - 2)\cos^2 \eta + 1][1 + (4M^4/k^4)\sin 2\eta]\}^{1/4}}{\{[2M^2 \cos^2 \eta - 1][1 + (4M^2/k^2)\cos 2\eta + (12M^4/k^4)\sin^2 2\eta]\}^{1/2}} \cos[kr \cos(\chi + \eta)], \tag{21}$$

where $\chi$ as a function of $\eta$ is determined by Eq. (20) and $k$ is defined by Eq. (9).

The geometric form of the wave crest surfaces can be easily found in the following way. Obviously, such a surface can be obtained by the rotation of its cross section by the $(x,y)$ plane around the $x$ axis. Then we find from Eqs. (6), (9), and (20) the parametric formulae for the coordinates of this cross section as follows:

$$x = \frac{4s}{k^3} \cos \eta (1 - M^2 \cos 2\eta), \quad y = \frac{4s}{k^3} \sin \eta (2M^2 \cos^2 \eta - 1), \tag{22}$$

where $s = kr \cos(\chi + \eta)$ is the phase constant along the crest line. These formulae are identical to ones obtained in 2D case [10,11] which is natural since the Bogoliubov dispersion law for linear waves is the same for both two and three dimensions. However, the amplitude of waves as a function of the distance $r$ and the polar angle $\chi$ (or $\eta$) in 3D theory differs from that in the 2D case; now it decays with $r$ as $r^{-1}$ to satisfy the energy conservation law.

As is clear from Eq. (9), wave pattern (22) corresponds to the range of the parameter $\eta$,

$$-\arccos(1/M) \le \eta \le \arccos(1/M), \tag{23}$$

with the coordinates located outside the Mach cone defined by the relation

$$\sin \chi_M = \frac{1}{M}. \tag{24}$$

In particular, the small values of $\eta$ correspond to the waves located in front of the obstacle,

$$x \cong -\frac{s}{2\sqrt{M^2 - 1}} + \frac{(2M^2 - 1)s}{4(M^2 - 1)^{3/2}} \eta^2, \quad y \cong \frac{(2M^2 - 1)s}{2(M^2 - 1)^{3/2}} \eta, \tag{25}$$

i.e., the wave crest lines take here a parabolic form

$$x(y) \cong -\frac{s}{2\sqrt{M^2 - 1}} + \frac{(M^2 - 1)^{3/2}}{(2M^2 - 1)s} y^2. \tag{26}$$

The boundary values $\eta = \pm \arccos(1/M)$ correspond to the lines

$$\frac{x}{y} = \pm\sqrt{M^2 - 1}, \tag{27}$$

i.e., far from the obstacle, they approach the straight lines parallel to Mach cone (24). In the region in front of the obstacle where $y = z = 0$ and $x < 0$, we have $\eta = 0$; hence

$$k = 2\sqrt{M^2 - 1} \tag{28}$$

and the wavelength

$$\lambda = \frac{2\pi}{k} = \frac{\pi}{\sqrt{M^2 - 1}} \tag{29}$$

is constant. Equation (21) is reduced here to a simple formula

$$\delta n = \frac{2V_0}{\pi|x|}\sqrt{\frac{(M^2 - 1)(4M^2 - 1)}{(2M^2 - 1)(8M^2 - 1)}}\cos(2\sqrt{M^2 - 1}\,x). \tag{30}$$

The formulae are greatly simplified also in a highly supersonic limit and not too close to the Mach cone when $M\cos\eta \gg 1$. In this case Eq. (16) yields

$$\chi \cong \pi - 2\eta - \frac{\sin 2\eta}{2M^2}, \tag{31}$$

and even the leading order approximation $\chi \cong \pi - 2\eta$ gives good enough approximation in the most important region of the wave pattern. In particular, we get the expressions for the wave crest line,

$$x = \frac{s}{2M}(\tan^2\eta - 1), \quad y = \frac{s}{M}\tan\eta, \tag{32}$$

that is,

$$x(y) \cong -\frac{s}{2M} + \frac{M}{2s}y^2, \tag{33}$$

which is the limit $M \gg 1$ of Eq. (26). Density disturbance (21) takes the form

$$\delta n \cong \frac{V_0}{\pi r}\cos[M(r - x)], \quad M\cos\eta \gg 1, \tag{34}$$

and in front of the obstacle where $x = -r = -|x|$ it corresponds to the limit $M \gg 1$ of Eq. (30).

## III. NUMERICAL SIMULATIONS AND DISCUSSION

In our numerical simulations we have used the GP equation in the form

$$i\hbar\frac{\partial\psi}{\partial t} = -\frac{\hbar^2}{2m}\Delta\psi + V(\mathbf{r}, t)\psi + NU_0|\psi|^2\psi, \tag{35}$$

where

$$U_0 = 4\pi\hbar^2 a_s/m \tag{36}$$

is the effective interatomic coupling constant, with $a_s$ being the s-wave scattering length of atoms and $N$ is the number of atoms in the condensate so that $\psi$ is normalized to unity. This equation was transformed to nondimensional units in the following way. We take some $a_0 = \sqrt{\hbar/m\omega_x}$ as a unit of length and $\omega_x^{-1}$ as a unit of time (if the BECs were confined in a parabolic trap then $a_0$ would have a meaning of the "oscillator length" and $\omega_x$ of the oscillator frequency along the $x$ axis; however in our simulations the trap has a form of a box with impenetrable walls rather than of a parabolic potential; therefore, $\omega_x$ can be chosen arbitrarily for numerical convenience) and introduce

$$\tilde{t} = t\omega_x, \quad \tilde{\mathbf{r}} = \mathbf{r}/a_0, \quad \tilde{\psi} = \psi \times a_0^{3/2},$$

$$\tilde{V} = V/(m\omega_x^2 a_0^2), \quad g = 4\pi a_s N/a_0, \tag{37}$$

so that the nondimensional GP equation assumes the form

$$i\frac{\partial\psi}{\partial t} = -\Delta\psi + V(\mathbf{r}, t)\psi + g|\psi|^2\psi, \tag{38}$$

with tildes omitted for convenience of the notation.

In the current simulations the BEC was confined in a cubic box $-10 \le x, y, z \le 10$ and had practically uniform undisturbed distribution of the density $n_0 = |\psi|^2 = 1.5714 \times 10^{-4}$ except for a narrow region at the boundary of the box. The other parameters have been chosen so that $g = 8000$, the sound velocity $c_s = \sqrt{gn_0} = 1.1212$, and the healing length $\xi = 1/(\sqrt{2}c_s) = 0.6307$. The potential of the obstacle was represented by a spherical ball with the radius $a_{ball} = 0.125$ (which is less than the healing length) and the repulsive uniform potential equal to $V_{ball} = 100$ inside the sphere. The velocity of the ball corresponds to the Mach number equal to $M = 3$. In our simulations we have used the method of lines with spatial discretization by the Fourier pseudospectral method and time integration by the adaptive Runge-Kutta method of orders 2 and 3 (RK23).

The resulting wave pattern is shown in Fig. 2. We have found that it is axially symmetric, as it was supposed, and the $(x, y)$ cross sections of the wave crest surfaces agree very well with the analytical curves shown by dashed lines and corresponding to Eq. (22). The profile of the density oscillations in front of the obstacle as a function of the $x$ coordinate is shown in Fig. 3 and it is compared with analytical expression (30). Again, a good agreement is observed almost everywhere except for the nearest vicinity of the potential where the wave is nonlinear, and our perturbation theory cannot be applied here. In particular, the "hole" in the condensate density behind the obstacle is not described by the present asymptotic theory which is correct far enough from the obstacle only. With the account of these reservations, the wave pattern located outside the Mach number is described quite well by the theory developed here.

Since the size of the obstacle is less than the healing length, there was no formation of vortex rings located inside the Mach cone. Just these structures attracted earlier much attention in the study of the loss of superfluidity in a sub-
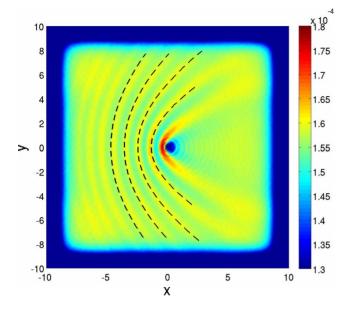
FIG. 2. (Color online) Numerically simulated wave pattern generated by a spherical obstacle moving through a Bose-Einstein condensate. The parameters of the BEC are indicated in the text. The analytical wave crest lines are shown by dashed lines. These are plotted according to Eq. (22).
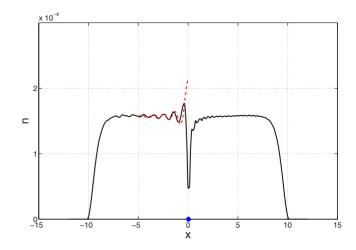


FIG. 3. (Color online) Oscillatory structure in front of the obstacle obtained by numerical simulations (solid line) and analytically [Eq. (30)]; dashed line). Position of the obstacle is shown by a dot.

sonic motion of obstacles (see, e.g., [17] and references therein) when the stationary "ship wave" patterns do not exist—in the subsonic case only the time-dependent linear waves can be generated due to the switching on the obstacle potential [18] or the change in the obstacle velocity. Similar vortex-antivortex pairs are also generated in the 2D case where they align along straight lines as the velocity of the obstacle grows, and above some critical value of velocity one can see the formation of oblique dark solitons attached at one end to the obstacle and decaying into vortices at the other end. One may suppose that if the size of the obstacle exceeds the healing length, then in the 3D case formation of "conical solitons" would take place above some critical velocity. However, the study of this problem is outside the scope of the present paper.

In conclusion, we have studied the formation of the linear wave pattern generated by a 3D small obstacle moving with a supersonic velocity through a uniform condensate. Analytical formulae for the wave crest lines and the dependence of the amplitude of the density oscillations on the distance from the obstacle are confirmed by numerical simulations. This theory essentially extends previous calculations of the "drag force" and provides a more detailed picture of the process of Cherenkov radiation of Bogoliubov excitations in rarefied Bose condensates. One may hope that the predicted wave structures can be observed experimentally.

## ACKNOWLEDGMENTS

[1] L. D. Landau, J. Phys. (USSR) **5**, 71 (1940).

[2] L. D. Landau, J. Phys. (USSR) **11**, 91 (1947).

[3] R. P. Feynman, in *Progress in Low Temperature Physics*, edited by C. J. Gorter (North-Holland, Amsterdam, 1955), Vol. I, p. 17.

[4] D. L. Kovrizhin and L. A. Maksimov, Phys. Lett. A **282**, 421 (2001).

[5] G. E. Astrakharchik and L. P. Pitaevskii, Phys. Rev. A **70**, 013608 (2004).

[6] E. A. Cornell, *Conference on Nonlinear Waves, Integrable Systems and their Applications*, Colorado Springs, CO, June 2005 (http://jilawww.colorado.edu/bec/papers.html).

[7] I. Carusotto, S. X. Hu, L. A. Collins, and A. Smerzi, Phys. Rev. Lett. **97**, 260403 (2006).

[8] A. Amo, J. Lefrère, S. Pigeon, C. Adrados, C. Ciuti, I. Carusotto, R. Houdré, E. Giacobino, and A. Bramati, e-print arXiv:0812.2748.

[9] T. Winiecki, J. F. McCann, and C. S. Adams, Phys. Rev. Lett. **82**, 5186 (1999).

[10] Yu. G. Gladush, G. A. El, A. Gammal, and A. M. Kamchatnov, Phys. Rev. A **75**, 033619 (2007).

[11] Yu. G. Gladush, L. A. Smirnov, and A. M. Kamchatnov, J. Phys. B: Mol. Opt. Phys. **41**, 165301 (2008).

[12] G. A. El, A. Gammal, and A. M. Kamchatnov, Phys. Rev. Lett.

**97**, 180405 (2006).

[13] G. A. El, Yu. G. Gladush, and A. M. Kamchatnov, J. Phys. A: Math. Theor. **40**, 611 (2007).

[14] A. M. Kamchatnov and L. P. Pitaevskii, Phys. Rev. Lett. **100**, 160402 (2008).

[15] Yu. G. Gladush, A. M. Kamchatnov, Z. Shi, P. G. Kevrekidis, D. J. Frantzeskakis, and B. A. Malomed, Phys. Rev. A **79**,

033623 (2009).

[16] R. G. Scott and D. A. W. Hutchinson, Phys. Rev. A **78**, 063614 (2008).

[17] N. G. Berloff and P. H. Roberts, J. Phys. A **33**, 4025 (2000).

[18] B. B. Baizakov, A. M. Kamchatnov, and M. Salerno, J. Phys. B **41**, 215302 (2008).